Report titled

Afferent Feedback Predicts Effort Expenditure In Human Locomotion :

A NEUROMUSCULAR MODELING STUDY

submitted in partial fulfillment of the requirements of

BTECH MECHANICAL ENGINEERING

by

Anushree Sabnis (191021056)

2022-23

Under the Guidance of

Dr. Raju M. Tayade

MECHANICAL ENGINEERING DEPARTMENT

VEERMATA JIJABAI TECHNOLOGICAL INSTITUTE

MATUNGA, MUMBAI - 400019

ACADEMIC YEAR 2022-23

DECLARATION OF CANDIDATE

I declare that this written submission represents my ideas in my own words and where others' ideas or words have been included, I have adequately cited and referenced the original sources.

I also declare that I have adhered to all principles of academic honesty and integrity and have not misrepresented or fabricated or falsified any idea / data / fact / source in my submission.

I understand that any violation of the above will be cause for disciplinary action by the Institute and can also evoke penal action from the sources which have thus not been properly cited or from whom proper permission has not been taken when needed.

Signature of candidate
Anushree Sabnis
Roll No: 191021056

Date: 09 / 06 / 2023
Place: Veermata Jijabai Technological Institute, Mumbai

STATEMENT OF CANDIDATE

I wish to state that work embodied in this report titled "**Afferent Feedback Predicts Effort Expenditure In Human Locomotion : a neuromuscular modeling study"** forms my to the work carried out under the guidance of Dr. Raju M. Tayade at Veermata Jijabai Technological Institute. This work has not been submitted for any other Degree or Diploma of any University/Institute. Wherever references have been made to the previous works of others, it has been clearly indicated.

Signature of candidate
Anushree Sabnis
Roll No: 191021056

Date: 09 / 06 / 2023
Place: Veermata Jijabai Technological Institute, Mumbai

APPROVAL SHEET

CERTIFICATE

This is to certify that **Anushree Sabnis (191021056)**, a student of **B.Tech. Mechanical Engineering**, has completed the report entitled, "**Afferent Feedback Predicts Effort Expenditure In Human Locomotion : a neuromuscular modeling study"** to our satisfaction.

Dr. Raju M. Tayade

Guide / Supervisor

Dr. W. S. Rathod

Head of Department - Mechanical Engineering

Dr. Sunil Bhirud

Director, VJTI

CERTIFICATE

The report titled "**Afferent Feedback Predicts Effort Expenditure In Human Locomotion : a neuromuscular modeling study"** submitted by **Anushree Sabnis (191021056)**, is found to be satisfactory and is approved for the Degree of **B.Tech. Mechanical Engineering**

Dr. Raju M. Tayade

Supervisor / Guide **Examiner**

Date: 09 / 06 / 2023 Place: Veermata Jijabai Technological Institute, Mumbai

CONTENTS

LIST OF TABLES

LIST OF FIGURES

ABSTRACT

Humans have a preference towards walking at economical speeds (ES) which minimise metabolic energy consumption. However, it is unclear what sensory information the nervous system uses to evaluate the energetic cost of a given behavior. Few studies have been able to map afferent feedback from individual lower-limb muscle proprioceptors to modulation of effort in steady-state gait. This study investigates if proprioceptive feedback could be used to estimate energy consumption during human gait through neuromechanical simulations. Specifically, 27 afferent feedback signals of active fibre force, contractile velocity and muscle fibre length are considered. A musculoskeletal model with a reflex-based controller was used to generate simulations of human gait over slow and fast speeds, and optimised to modulate the metabolic cost of transport to express normal and elevated range of costs. We developed a metamodel mapping afferent feedback signals to effort modulation using Partial Least Squares Regression (PLSR) as a dimensionality reduction technique. We also estimated the metabolic cost of transport (CoT) of walking using this PLSR metamodel. Furthermore, we predicted gait characteristics such as the economical speed (ES) using this estimated value of CoT. We validated our predictions using model accuracy metrics and statistical tests of significance. Our results indicate that the peripheral nervous system may regulate unperturbed gait through afferent feedback factors related to muscle force generation in skeletal muscles.

CHAPTER 1: INTRODUCTION

1.1 Motivation of the Project

Humans prefer to walk in energetically economical ways. In order to achieve this, humans select gait characteristics such as speed, stride length, and stride frequency so as to minimise metabolic cost during steady-state walking (Zarrugh, M. Y., et al., 1974), (Bertram, J.E., 2005), (Faraji et al., 2018), (Donelan, J. M. et al., 2002). They also dynamically adapt their gait pattern to reduce energy cost when using devices such as exoskeletons and split-belt treadmills (Selinger et al., 2015), (Sanchez et al., 2021), (Sanchez et al., 2019), (Price et al., 2023). While it is evident that humans minimise the cost of transport (CoT) during walking in order to produce a stable gait, it is undetermined how our bodies gauge metabolic cost on a muscular level. In a recent study, the velocity feedback of the tibialis anterior muscle has been shown to act as an indirect physiological sensor of walking economy through predicting ground collisions and the associated energy transfer (Kwak & Chang, 2023). However, due to the complexity of neural mechanisms modulating gait, there is a lack of models mapping proprioceptive feedback from various skeletal muscles directly to measures of walking economy. The question remains to be addressed : which sensory feedback signals does the nervous system use to facilitate the minimization of metabolic energy expenditure during walking?

1.2 Literature Survey

To help minimise energetic cost, the nervous system needs a way to sense or estimate it. There are various ways in which the nervous system could use sensory feedback to estimate effort. Every voluntary action is associated with a subjective “sense of effort”. A majority of research attributes the neural origins of this sense to either central or peripheral signals. Central mechanisms involving cerebellum-dependent internal models are hypothesised to contribute to the “sense of effort” through

comparing efference copies to reafference signals encoding muscle force information. An internal model, as reviewed in (Wolpert et al., 1998) and (Kawato, 1999), is a theoretical neural system emulating interactions among subsystems involved in motor control such as the CNS, and between the body and the environment. It is generally acknowledged that efference copies, which are internal copies of motor commands, contribute to effort perception (Miall et al., 1993; (Gandevia & McCloskey, 1977a; Gandevia & McCloskey, 1977b). The internal model is also postulated to combine efferent and afferent signals from CNS and PNS respectively to estimate the sense of effort (Sanes & Shadmehr, 1995), (Lafargue et al., 2003). There are contrasting hypotheses which describe the contribution of the peripheral nervous system in the "sense of effort" as either through physiological sensors (such as blood-gas chemoreceptors) or through muscle proprioception. An abstract representation of energetic cost measured by a physiological sensor could be used to track metabolic cost. However, in their recent work, Wong et al., (2017) concluded that blood-gas receptors are an unlikely physiological sensor for the whole-body energy expenditure and raised the possibility of a muscle-level sensor for metabolic cost. Muscle-level sensors transmit proprioceptive information from muscle spindles to the CNS at varying degrees of accuracy and speed. Myelinated group I and II afferents are specialised fast-conducting sensory neurons carrying precise information regarding muscle length, velocity and joint position changes for both static and dynamic proprioception. On the other hand, thin unmyelinated group III and IV afferents (C fibres) are polymodal and inform the CNS (with high latency) about mechanical and metabolically induced stress, contributing to the sense of fatigue during exercise. Intrathecal or epidural injections of anaesthetics of analgesics, such as lidocaine or fentanyl, has traditionally been used to investigate the role of C fibres in cardio-respiratory responses to static exercise. These techniques involve pharmacologically blocking C fibres while monitoring the sense of effort. Results from these studies are conflicting, with different studies' results indicating decreased (Amann et al., 2008), unchanged (Barbosa et al., 2016), (Smith et al., 2003) or increased (Kjær et al., 1989) perception of effort. Unlike this, recent studies involving bilateral weight-matching (BL Luu et al., 2011) and mapping fascicle dynamics to modulation of CoT during steady-state walking (Kwak & Chang, 2023) have shown that primary and secondary spindle afferents play a major role in effort perception.

Muscle proprioceptors, such as muscle spindles and golgi tendon organs(GTO), are innervated by sensory afferent neurons transmitting signals encoding skeletal muscle dynamics such as muscle

length, contractile velocity, joint position and muscle tension, as described above. Umberger et al.'s (2003) seminal work on modelling human muscle energy expenditure describes the role of muscle proprioceptive feedback in the computation of the total rate of muscle energy expenditure. From an energy liberation perspective, the rate of muscle energy expenditure can be categorised into the total heat liberation rate (activation, maintenance and shortening heat liberation) and the mechanical work rate of the contractile element, all of which are dependent on proprioceptive afferent feedback such as muscle fiber length, contractile velocity and active fiber force. The neuronal control of locomotion, specifically somatosensory feedback from the legs for proprioception or indicating movement or position of the leg, is hypothesised to be necessary to regulate human locomotion at all speeds (Akay, T.; Murray, A.J., 2021). Proprioceptors could thus be considered as indirect biophysical sensors encoding effort perception information. There are two reasons to suspect this. Firstly, the muscle's capacity to generate force and its energetic efficiency is the highest at intermediate shortening velocity. This is due to the force-velocity interrelation, as the muscle's force generation decreases on increase of contractile velocity in a hyperbolic manner (Hill, A; 1938). This alludes to the possibility that the maximal active fibre force and maximal contractile velocity may have an impact on the metabolic energy consumption through regulating the muscle's force generation capabilities. Secondly, the efficiency of force generation of a muscle depends on the type of contraction that it is undergoing. Muscles require less metabolic energy to generate force when they are active isometrically than when they perform work in a contracted state (Fenn, W.; 1924) . This suggests that the relative contraction against resting muscle length regulates the force generation and energy consumption of a muscle.

1.3 Literature Gap

In this study, we aim to investigate the role of proprioceptive afferent feedback in energy expenditure through a metamodel mapping afferent feedback signals of fiber length, velocity and force to effort modulation. We have extended upon our previous work which usedusing a parameter-sweep approach through computational modelling to find key reflex parameters modulating gait characteristics; with neuromechanical simulations optimised to minimise COT at self-selected speeds (Di Russo et al., 2021). This approach has been previously used to test reflex-based controllers for human locomotion (Geyer H, Herr H., 2010), (Ong CF et al., 2019). We generated computer simulations of steady-state human locomotion at a range of speeds and energy expenditures, and recorded muscle length,

contractile velocity and active fiber force afferent feedback signals from each simulation. The three time-varying afferent feedback signals were reduced to three representative time-invariant scalar afferent feedback factors per simulation. Key afferent feedback factors were isolated through correlational and regression analyses with the minimised effort. We then developed a metamodel mapping parametric variations in key afferent feedback factors to variations in state variables describing energetic expenditure. We employed Partial Least Squares Regression (PLSR) as a model reduction technique to generate the mappings. Modelling strategies and regression discontinuities over the entire dataset of gait across speed and effort ranges was evaluated through the Chow test. The PLSR model and its predictions were cross-validated. The model's capability to predict the minima of the CoT-speed curve observed in literature was evaluated through cross-validation, model accuracy metrics and statistical tests of significance.

We aim to understand the possible mechanisms of effort modulation in human locomotion through afferent feedback factors. We address the following questions :

- Are afferent feedback signals pivotal for effort modulation during human gait?
- Can afferent feedback signals be used to estimate the metabolic energy expenditure during human locomotion?
- Can afferent feedback signals be used to estimate the economical speed (ES) of walking, i.e. the minimum cost of transport expressed as a function of walking speed (CoT(v)) ?

CHAPTER 2 : REPORT OF THE PRESENT INVESTIGATION (METHODOLOGY)

2.1 Methods

We used a forward-shooting optimization method to generate simulations of human walking. Our model was implemented using the Hyfydy physics engine (Geijtenbeek, 2021), and the gait controller and locomotion costs were implemented in the SCONE (Geijtenbeek, 2019) optimization framework. The SCONE simulation comprises a musculoskeletal model, controller, cost function composed of several cost components, and an optimizer that optimises the initial conditions and controller parameters to minimise the cost function.

2.2 Musculoskeletal model

The musculoskeletal model (Figure 1) used was a planar model, based on a previous model representing an adult with a height of approximately 1.8m and a mass of 74.53 kg (Delp et al., 1990). The musculoskeletal model had 9 degrees of freedom (dof), with a 3 dof planar joint between the pelvis and ground constraining the model in the sagittal plane. 1 dof revolute joints represented the hip, knee and ankle of each leg. A compliant contact model as described in (Hunt & Crossley, 1975) was used to model the interactions between the feet and the ground, represented by contact spheres and contact planes. Each foot had 2 contact spheres of radius 3 cm, one each representing the heel and the toes, and a contact half space plane representing everything above the ground plane.

The model is actuated with 9 Millard-optimised Hill-type muscles per leg : gluteus maximus (GMAX), biarticular hamstrings (HAMS), iliopsoas (ILPSO), rectus femoris (RF), vasti (VAS), biceps femoris short head (BFSH), gastrocnemius (GAS), soleus (SOL) and tibialis anterior (TA). The optimised

implementation of the Hill-type muscle model, as described in (Millard et al., 2013), was used, which includes a passive damping term that allows velocity to be determined even when the muscle is deactivated.

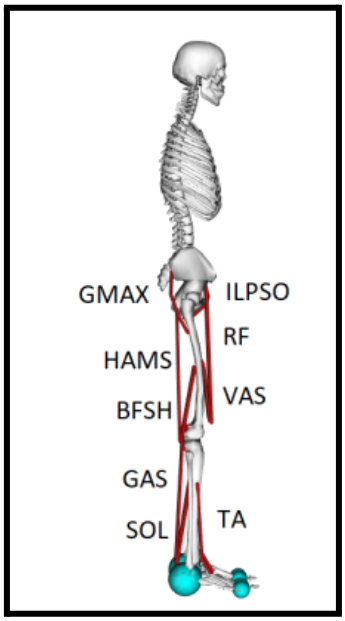

Figure 1 : Musculoskeletal model used to study human locomotion. The model is constrained in the sagittal plane and has 9 DoFs: hip and knee flexion/extension, ankle plantar/dorsal flexion for each leg, and a 3-DoFs planar joint between the pelvis and the ground. Movements are generated by the activation of 9 muscles per leg: gluteus maximus (GMAX), biarticular hamstrings (HAMS), biceps femoris short head (BFSH), rectus femoris (RF), iliopsoas (ILPSO), vasti (VAS), gastrocnemius medialis (GAS), soleus (SOL), and tibialis anterior (TA).

2.3 Reflex Controller

The model was controlled using the reflex controller proposed by (Geyer H, Herr H., 2010). The excitation of each muscle is governed by a simple state machine that switches states according to

different phases of the gait cycle, triggered by ground detection of the contact sensors described in the previous section. The controller employs three types of feedback mechanisms: Excitatory and Inhibitory Force Feedback from the Golgi tendon organs directed at muscle actions; the length and velocity feedback from muscle spindles that is active only during eccentric contraction to account for passive changes in muscle state; and the Proportional-Derivative (PD) gain feedback to maintain trunk orientation. A constant feedforward stimulation dependent only on the state of the gait cycle is also integrated into the muscles' stimulation to ADD RATIONALE HERE. The various types of stimulation provided to the muscles through these feedback mechanisms are mathematically described below :

Feedforward stimulation :

$$u_c = K_c \tag{1}$$

Stretch Feedback :

$$u_l = max(0, K_l(\bar{l}\,(t - t_D) - l_0)) \tag{2}$$

Force Feedback :

$$u_f = K_f . \bar{f}\,(t - t_D) \tag{3}$$

PD Balance feedback :

$$u_{PD} = K_P(\theta(t - t_D) - \theta_0) + K_V . \dot{\theta}\,(t - t_D) \tag{4}$$

Where, is constant, are the gains of the reflex controller, and is the length offset of the stretch response. The length offset defines the threshold value of the muscle length after which the length

feedback produces a stimulation to the muscle. is the desired forward lean angle regulating the proportional feedback of the actual forward lean angle . Delays are dependent on the muscle proximity to the vertebral column and are for the hip, knee and ankle respectively. For reflexes directed towards GMAX, ILPSO, HAMS and RF ; for reflexes directed towards BFSH and VAS and for GAS, SOL and TA . for each reflex was assigned on the basis of the most proximal joint that is crossed by the muscle towards which the reflex is directed. (For example, for the F+ reflex directed from HAMS to BFSH,)

2.4 Optimizations

SCONE was used as an optimization framework, and to formulate the model's state equations, controller and movement objective. 18 initial skeletal states were set by free parameter optimization. Muscle states were updated in each timestep according to the gains set in the controller, and were subsequently optimised and fed back to the system for integration till the desired time or till the model fell. To evaluate the modulation of effort at self-selected speeds, we defined an objective function P that we sought to minimise.

$$p = w_{speed} \cdot p_{speed} + w_{joint} \cdot p_{joint} + w_{grf} \cdot p_{grf} + w_{effort} \cdot p_{e\_dot} \quad (5)$$

The objective function was formulated to minimise the metabolic rate () while meeting predefined speed conditions, avoiding overcoming joint excursion limits, and maintaining head stability to avoid falling (eq. 6.). Individual components of the cost function are further described below :

1. p_{speed} is the penalty to minimise deviation from a predefined speed range and acts as a failsafe to ensure gait stability. This penalty returns a value between 0 (when speed conditions are met) and 1 (model falls over immediately). The value of this penalty represents the deviation of current speed from the speed range, normalised by the minimal viable speed. An additional constraint represents the threshold below which the current height of the centre of mass (COM) of the model with respect to the initial height of the COM would lead to unstable gait.

$$p_{speed} = \begin{cases} w_{speed}.\left(1 - \frac{|v_{model} - v_{min}| + |v_{max} - v_{model}|}{v_{min}}\right) & \frac{H}{H_0} > h_{max} \\ 1 & \frac{H}{H_0} < h_{max} \end{cases} \quad (6)$$

2. p_{joint} penalises deviation of instantaneous joint-level variables from a desired range. It was added into the objective function to prevent excessive knee torque and prevent ankle overextension. Desired joint ranges are defined as [-60,60] degrees for the ankle and [0,0] Nm for the knee.

$$p_{joint} = w_{joint}.|j_{model} - j_{range}| \quad (7)$$

3. p_{effort} is computed as the total rate of metabolic energy consumption over all muscle tendon units (MTU) normalised to distance travelled and mass. We used the model for metabolic energy consumption described in (Anderson, 1999) with updates from (Bhargava et al., 2004) and (Wang et al., 2012). The rate of metabolic energy consumption is the sum of the mechanical work rate performed by the muscle and the rate of heat released due to activation, maintaining contraction and shortening. It is quantified as follows :

$$\dot{E} = \dot{A} + \dot{M} + \dot{S} + \dot{W} \quad (8)$$

Where $\dot{A}$ represents the muscle activation heat rate, $\dot{M}$ is the muscle maintenance heat rate, $\dot{S}$ is the shortening heat rate and $\dot{W}$ is the mechanical work rate.

The total p_{effort} term is expressed as the cost of transport, using the cumulative sum of metabolic energy expenditure rate over all MTUs as follows :

$$p_{effort} = \frac{\dot{B} + \frac{1}{T}.\sum_{t=1,m\in M}^{T} \dot{E}_{m,t}}{distance.mass_{model}} \quad (9)$$

Where $\dot{B}$ is the basal energy computed as $1.5.mass_{model}$ according to (Wang et al., 2012).

The Covariance Matrix Adaptation Evolution Strategy (CMA-ES) method is used to optimise the parameters and obtain different walking behaviours. The optimization parameters are the maximum number of generations after which to stop the simulation equal to 100000 and the minimum progress after which to stop the optimization equal to 0.0001.

2.5 Optimization Sets

To understand how proprioceptive signals are varied with energy cost, we generated a range of feasible gaits by minimising and maximising the objective function for each target walking speed, with target speeds ranging from slow to fast gait. The two optimization sets in which the objective function is minimised and maximised are referred to as MINIMISATION set and MAXIMISATION set respectively. The assigned weights of components of the simulation objectives described in Section 2.3 for the optimization and validation sets are described in Table 1, along with the observed self-selected speed ranges.

Table 1 : Assigned weight for each component of the cost function for the two optimization sets i.e. MINIMIZATION set and MAXIMIZATION set

	MINIMIZATION set	MAXIMIZATION set
w_{effort}	0.1	-0.1
w_{joint}	[ankle : 0.1, knee : 0.01]	[ankle : 0.1, knee : 0.01]
w_{speed}	100	100
w_{grf}	1	1

2.6 Afferent feedback signal processing

Afferent information from muscles communicate information about muscle stretch via group Ia and group II afferents innervating the muscle spindles; and tendon tension, which is a measure of force or load on the muscle tendon unit transmitted by the Ib afferents innervating the golgi tendon organs (Wall, P.D.; Dubner, R., 1972)

We determined the force generated by the muscle, contractile element velocity and muscle fibre length as three important physiological variables that could be processed to estimate the rate of metabolic energy consumption due to muscle activity. Affrent feedback signals over a 10-second simulation are represented mathematically as follows :

$$\begin{aligned} \tilde{L}_M(t) &: Muscle\ fiber\ length \\ \tilde{F}_M(t) &: Muscle\ active\ fiber\ force \\ \tilde{V}_M(t) &: Contractile\ element\ velocity \end{aligned} \tag{1}$$

The afferent feedback signals for each experiment are smoothed using a 3rd order polynomial Savitzky-Golay filter of window length 0.1 second. The above mentioned three afferent feedback signals (Equation 10.) are extracted and smoothed for each of the 9 muscles in each leg. We thus consider 27 smoothed candidate afferent feedback signals per leg for each simulated experiment ($S \in \mathbb{R}^{27 \times T}$), represented as follows :

$$\tilde{F}_{GMAX}, \tilde{F}_{HAMS}, \tilde{F}_{BFSH}, \tilde{F}_{RF}, \tilde{F}_{ILPSO}, \tilde{F}_{VAS}, \tilde{F}_{GAS}, \tilde{F}_{SOL}, \tilde{F}_{TA}$$

$$\tilde{L}_{GMAX}, \tilde{L}_{HAMS}, \tilde{L}_{BFSH}, \tilde{L}_{RF}, \tilde{L}_{ILPSO}, \tilde{L}_{VAS}, \tilde{L}_{GAS}, \tilde{L}_{SOL}, \tilde{L}_{TA}$$

$$\tilde{V}_{GMAX}, \tilde{V}_{HAMS}, \tilde{V}_{BFSH}, \tilde{V}_{RF}, \tilde{V}_{ILPSO}, \tilde{V}_{VAS}, \tilde{V}_{GAS}, \tilde{V}_{SOL}, \tilde{V}_{TA}$$

We then investigated the impact of afferent feedback signals on the estimation of effort for a range of speeds.

2.7 Statistical Analyses

Simulations were carried out at speeds in the range [0.4, 1.6] m/s for both MINIMIZATION and MAXIMIZATION optimisation sets. Afferent feedbacks

We then selected an optimal PLSR model and modeling strategy to estimate the metabolic rate, CoT and economical speed (E.S.), and validated our prediction accuracy using tests of significance as well as model accuracy metrics. Finally, we analyzed the loadings of the identified key afferent feedback factors in the PLS components through graphical means. The detailed methodology of these analyses are described further in sections below.

2.8 Predictive Analysis : Selection of Optimal PLSR model

We aimed to determine whether the 27 afferent feedback signals could be used to estimate :

a. Rate of Metabolic energy expenditure ($\dot{E}$)
b. Minimum CoT and corresponding minimum speed

The dataset was prepared with 27 afferent feedback signals per simulation, combining 144 MINIMIZATION and 123 MAXIMIZATION sets. Thus, the dataset could be represented as NxTxF

$$X \in \mathbb{R}^{N \times S} \quad (1)$$

Where N is the total number of experiments and S is the set of 27 afferent feedback signals per simulation of 10 seconds.

Partial Least Squares Regression (PLSR) was used to model $\dot{E}$ using the afferent feedback signals, taking a randomly selected set of two-thirds of the available samples for modeling $\dot{E}$ and the remaining fourth for independently validating the model.

Leave-one-out validation was used to determine the optimal number of components (N_{opt}) to use in the PLSR model. For modeling $\dot{E}$, we tested up to 27 bilinear components. The accuracy of the cross-validation is given by the Root Mean Squared Error (RMSE). In order to avoid overfitting, N_{opt} with the lowest RMSE value was chosen when the curve of RMSE-N_{opt} more or less flattened.

2.9 Predictive Analysis : Validation of PLSR model predictions

An optimum number of PLS components ($\phi_{1:N_{opt}}$) was selected using the methods described in section 2.6. The PLSR model for the dataset was validated using K-fold cross-validation with 5 splits. The data is split into 5 roughly equal parts. The cross-validation predictions involved computing each N_{opt}-factor PLSR model using 4 out of a total of 5 split parts of data. The PLSR model regresses $\dot{E}$ on $\phi_{1:N}$, modeling the function $\dot{E}(\phi_{1:N})$ for for the 4 parts and predicting the $\dot{E}(\phi_{1:N})$ of the removed part of data. This is repeated for all 5 parts. The coefficient of determination for cross-validation (R^2-CV) was used to quantify explained variability of predictions as well as the goodness of fit. .

The quality of predictions expressed by R^2 is described as follows : $R^2 \geq 0.9$ indicates excellent model fit with low variance in predictions and high explained variability. $0.7 \leq R^2 \leq 0.9$ indicate good model fit with low variance in predictions and with lower explained variability compared to excellent fit. $R^2 \geq 0.9$ indicates good model fit with high variance in predictions but also high explained variability. $0.7 \leq R^2 \leq 0.9$ indicate moderate fit with high variance in predictions and comparatively lower explained variability.

The results of the 'validation' PLSR model were graphically visualized in a two-dimensional biplot (Oyedele & Lubbe, 2015), which superimposed $\phi_{1:N}$, which were orthogonal bilinear combinations of the 27 key afferent feedback factors pertaining to muscle force ($\tilde{F}_M$), length ($\tilde{L}_M$) and velocity ($\tilde{V}_M$) into one joint graphical display. A scaling method was used for the loadings of the 27 key afferent feedback factors in ϕ_1 and ϕ_2 prior to constructing the biplot.

2.10 Predictive Analysis : Predicting Minimum CoT and corresponding minimum speed

CoT shows a U-shaped curve as a function of walking speed (v), which includes the particular walking speed minimizing the CoT, referred to as 'economical speed $(E.S.)$. The experimental value of CoT (COT_{exp}) and the PLSR-estimated value of CoT $COT(\phi_{1:N})$ were calculated by dividing each individual measurement of $\dot{E}_{exp}$ and $\dot{E}(\phi_{1:N})$ respectively by the constant model mass and speed (v) at which it had been determined. Polynomial regression was performed on v to obtain quadratic functions $COT_{exp}(v)$ and $COT(\phi_{1:N}, v)$ for MINIMIZATION, MAXIMIZATION optimisation sets and their COMBINED dataset.

Significant differences between minimum values of $COT_{exp}(v)$ and $COT(\phi_{1:N}, v)$ as well as between $E.S.$ at $COT_{exp}(v)$ and $E.S.$ at $COT(\phi_{1:N}, v)$ were studied by performing two separate paired t-tests. Significance was set for both paired t-tests at $P < 0.05$.

All data analyses were accomplished using Python libraries Numpy, Scipy, Scikit-Learn.

CHAPTER 3 : RESULTS & DISCUSSIONS

3.1 Explorative Analysis Results

The range of speeds simulated across both optimization sets of metabolic effort MINIMIZATION and metabolic effort MAXIMIZATION is identified as [0.43, 1.60] m/s . The range of metabolic cost of transport and speed across the COMBINED dataset is reported in Table 2.

Table 2 : Range of metabolic cost of transport and speed observed in the MINIMIZATION, MAXIMIZATION optimization set and their COMBINED optimization set

Quantity	MINIMIZATION set	MAXIMIZATION set	COMBINED (MINIMIZATION and MAXIMIZATION) set
COT ($W\ kg^{-1}\ m^{-1}$)	[5.17, 10.18]	[6.49, 15.26]	[5.17, 15.26]
Speed ($m\ s^{-1}$)	[0.53, 1.60]	[0.43, 1.44]	[0.43, 1.60]

Upon comparing the metabolic energy expenditure computed across the effort MINIMIZATION and effort MAXIMIZATION optimization sets, we verify that a higher rate of metabolic effort consumption was reported in the latter (Figure 2) .

Figure 2 : Boxplot showing range of metabolic cost of transport (COT) – The energetic cost of travelling a given distance, over two sets of optimizations.

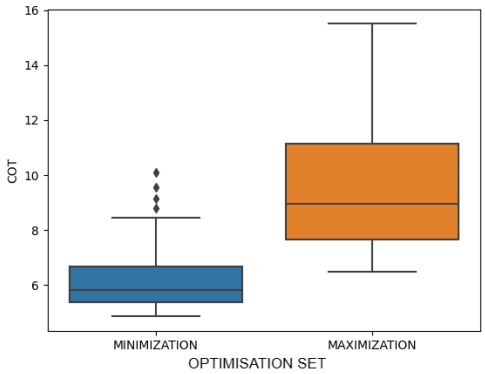

3.2 PLSR Model Selection

For model selection, a second-order polynomial PLSR using all the observations in the 'calibration' set was used with leave-one-out (L.O.O.) cross-validation. The PLSR model was then chosen according to the minimum cross-validated RMSE. N_{opt} for the model was 10 (Figure 3), so the 10-factor PLSR model was selected selected for the estimation of $\dot{E}$ and the statistically independent (cross-validated) predictions of $\dot{E}$ and COT.

Figure 3 : Partial least squares regression modelling and prediction output for $\dot{E}$ and COT in each of the MINIMIZATION, MAXIMIZATION and COMBINED optimisation sets. Columns: (a) shows the L.O.O. cross-validated root mean squared error (RMSE) of $\dot{E}$prediction against the number of factors (b) shows the Variance (%) explained by each component

(a) (b)

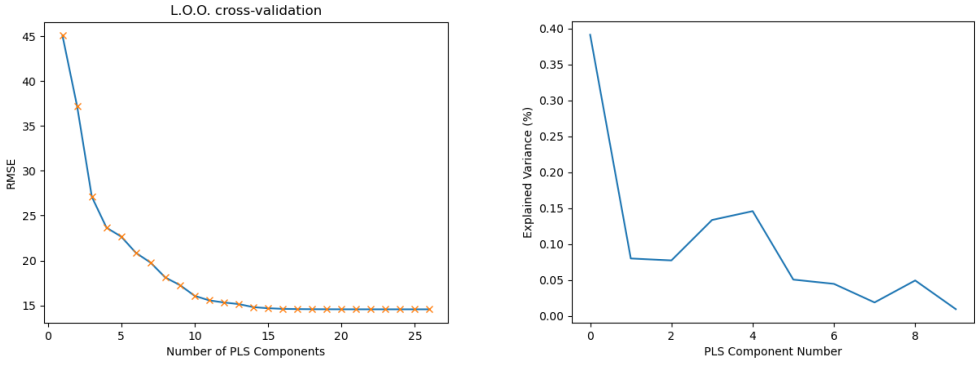

3.3 Validation of PLSR model predictions

PLSR using the highly linearly correlated key afferent feedback factors gave stable estimates for all submodels with excellent to good predictive ability. We have presented the cross-validation R^2 (R^2-CV) using the train set data as well as the statistically independent R^2 using the test set data for the combined dataset in Table 4.

For the 'train' set, for $\dot{E}$ and COT, the cross-validation R^2-CV is 0.924 and 0.863 respectively. Likewise for 'test' set, the cross-validation R^2-CV is 0.956 and 0.886 respectively (Table 4). No significant difference was observed in the accuracy metrics (RMSPE and R^2) between the 'calibration' and 'validation' sets, which verified that there was no overfitting of the model.

PLSR modeling thus gave us metamodels mapping variation in $\dot{E}$ and COT to variation in key afferent feedback factors; through the polynomial functions $\dot{E}(\phi_{1:10})$ and $COT(\phi_{1:10})$. The models described in this study for all sets are excellent fits ($R^2 > 0.9$), indicating that there is low variance in the predictions and high explained variance by the model.

Table 3 : Results of PLSR applied to $\dot{E}$ and COT a randomized selection of 'test' (75% of the data) and 'train' (25% of the data) sets the combined dataset.

Metabolic Function	R^2-CV (train)	R^2-CV (test)
$\dot{E}(\phi_{1:10})$	0.924	0.956
$COT(\phi_{1:10})$	0.863	0.886

3.4 Predicting minimum COT and corresponding E.S.

Predicted $COT(\phi_{1:N}, v)$ (obtained from PLSR predictions) and measured $COT_{exp}(v)$ (derived from recorded values of $\dot{E}_{exp}$) were best described by individual second-order polynomial regressions for each studied set (Figure 4). $E.S._{exp}$ and $E.S._{aff}$, recorded in Table 5, were calculated by determining the speed at which the first-order derivatives of $COT_{exp}(v)$ and $COT(\phi_{1:N}, v)$ were zero for each set.

The COMBINED set showed the lowest E.S., followed by the MINIMIZATION and MAXIMIZATION sets; whereas the lowest COT was observed in MINIMIZATION set, followed by the COMBINED and MAXIMIZATION sets (Table 5).

The test statistic of the paired t-test performed showed a p-value of 0.9542 between $E.S._{exp}$ and $E.S._{aff}$, and a p-value of 0.7882 between $COT_{exp}(v)$ and $COT(\phi_{1:N}, v)$. This is sufficient evidence to say that there is no significant difference between experimental values of E.S. and COT and estimated values of E.S. and COT using PLSR modeling. In other words, PLSR modeled on 27 afferent feedback signals can be used to predict the value of minimum COT as well as E.S.

Figure 4 : Cost of Transport versus speed for the 'validation' sets of COMBINED (blue), MINIMIZATION (orange) and MAXIMIZATION (green) sets. Curved lines represent the best fit for polynomial relationships of predicted COT against speed.

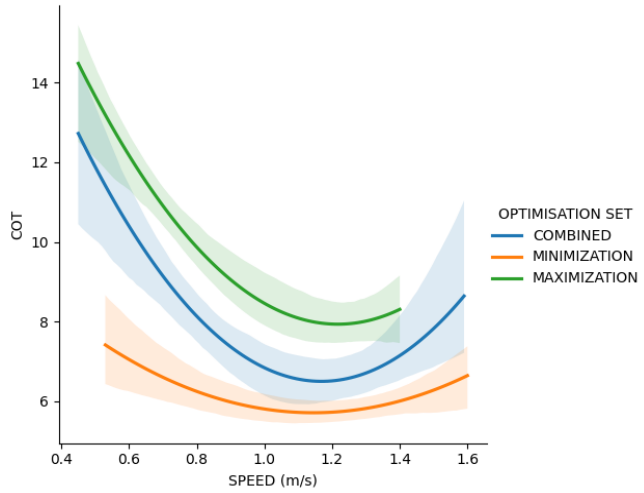

Table 4 : Economical speeds obtained from minima of COT(v) for calibration and validation subsets of MINIMIZATION, MAXIMIZATION optimisation set and their COMBINED set.

Optimisation set	$E.S._{exp}$ (ms^{-1}) for $COT_{exp}(v)$	$E.S._{aff}$ (ms^{-1}) for $COT(\phi_{1:N}, v)$	Paired t-test p-value
MINIMIZATION	1.1899	1.2020	0.9542
MAXIMIZATION	1.2901	1.2774	
COMBINED	1.166	1.168	

3.5 Primary proprioceptors for joint movement minimizing energy cost

The PLSR biplot for $\dot{E}(\phi_{1:10})$ for the combined dataset explained 68.5% of the interaction variance in the predictor variables (27 afferent feedback signals) with the first four PLS components (ϕ_1, ϕ_2 , ϕ_3 and ϕ_4). The PLSR biplot (Fig. 5) indicated that the interaction was most important in $\tilde{F}_{BFSH}$ and $\tilde{F}_{SOL}$; and less important in $\tilde{V}_{BFSH}$ and $\tilde{L}_{SOL}$, since the position of these vectors was closest to the biplot origin. Therefore, the major interactions in afferent feedback was due to the force feedback of the knee flexors and ankle plantar flexors.

Figure 5: PLSR Biplot of (a) (ϕ_1 - ϕ_2) and (b) (ϕ_3 - ϕ_4) explaining total of 68.5% of total variance in the dataset

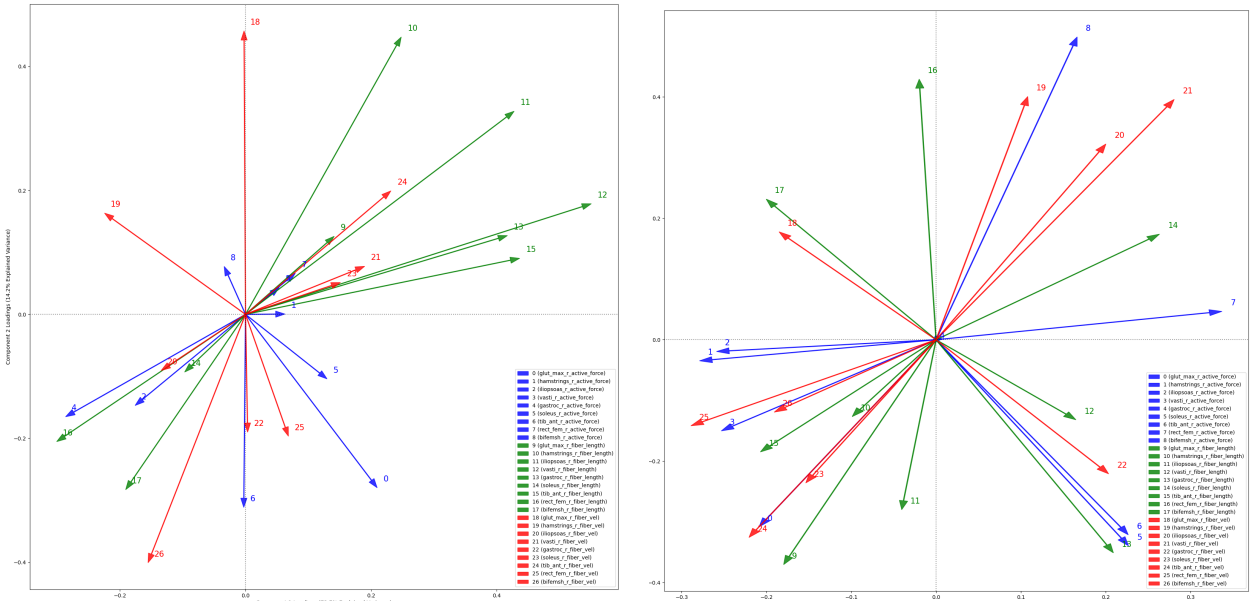

3.6 Discussion

In this study we aimed to understand how the nervous system estimates and predicts whole body energetics of walking. We approached this by investigating whether proprioceptive feedback could be used to model effort modulation during human gait. We proposed that a PLSR-generated metamodel of a linear combination of afferent feedback factors arising from muscle proprioceptors, specifically muscle spindles and GTO, can be used to estimate the metabolic energy expenditure during walking. We also investigated whether the metamodel could effectively map afferent feedback to the speed dependence of CoT, through predicting the ES.Our results demonstrated that afferent feedback factors linked to proprioceptive feedback could be used to model and estimate the metabolic cost of transport.

It is important to understand which MTUs produce the key afferent feedback factors, as this provides great insight into which muscles contribute the most to producing energetically optimal gait. Distal leg muscles such as soleus and gastrocnemius have compliant and long series elastic elements, and

therefore are well suited to reducing muscle fiber velocities because most of their MTU length change during locomotion is carried out through stretch and recoil of these elements (Roberts, 2002), (Ishikawa et al., 2007), (Lichtwark, 2007). More proximal muscles such as BFSH, ILPSO, GMAX, HAMS do not have these compliant series elastic elements (Ker, R. F., Alexander, R. M. & Bennet, M. B., 1988) and so must provide most of their contractile length changes from fiber length changes. Previous studies have predicted that these variations in tendon structure between distal and proximal leg muscles leads to less efficiency in power output at the hip and knee joints than the ankle joints (Sawicki, G. S., Lewis, C. L. & Ferris, D. P, 2009). Moreover, knee extensor and hip extensor muscles are likely to undergo muscle lengthening during early stance. These muscles absorb energy during the early stance phase. Our results agree with this hypothesis as they indicate that the sensory feedback parameters, primarily the fibre length and the force generated, associated with the more proximal muscles of the leg mentioned above, may have a stronger impact on the modulation of effort than those of the distal leg muscles, with the exception of the TA.

We identified TA as the only distal leg muscle whose proprioceptive feedback might be pivotal to effort modulation in human gait. While proximal leg muscles contribute to propulsive force generation and pendular energy transfer mechanisms during the various phases of human gait, the TA maintains ankle position throughout the gait cycle. Recent research has explored a curve-fitting approach to correlate skeletal muscle dynamics using the muscle activity of TA to locomotion energetics (Kwak & Chang, 2023).

Terrestrial animals increase their walking speed by increasing the activity of extensor muscles. When locomotion speed increases, there is a decrease in the stance phase duration whereas the swing phase duration remains relatively constant. Due to this, step cycle duration decreases. Furthermore, electromyogram (EMG) activity recordings from flexor and extensor muscles during locomotion of cats during different speeds revealed that with increasing speed, the EMG activity of mainly the extensor muscles increases accordingly (Pierotti et al., 1989). It is possible that the speed-dependent amplitude regulation of extensor activity is controlled by proprioceptive sensory feedback. Experiments with humans suggest that amplitude modulation of extensor activity during walking is regulated by proprioceptive feedback from the golgi tendon organs (innervated by Ib afferents) and from the muscle spindles through (innervated by group Ia,II afferents). (af Klint et al., 2010), (Grey et

al., 2004), (Sinkjaer et al., 2000). Coherent to these observations, we observed a curvilinear or U-shaped graph of key extensor afferent feedback factors expressed as a function of locomotor speed. The greatest magnitude of extensor afferent feedback stimulation occurred at the lowest and/or highest speeds. It is also interesting to note that this U-shaped relationship with speed is observed only in the key afferent feedback factors of the extensor muscles (GMAX, HAMS, SOL) and not in the flexor muscles, with the exception of the hip flexor muscles (ILPSO).

CHAPTER 4 : SUMMARY & CONCLUSIONS

4.1 Summary

This study investigates if proprioceptive feedback could be used to estimate energy consumption during human gait through neuromechanical simulations. Specifically, 27 afferent feedback signals of active fibre force, contractile velocity and muscle fibre length are considered. A musculoskeletal model with a reflex-based controller was used to generate simulations of human gait over slow and fast speeds, and optimized to modulate the metabolic cost of transport to express normal and elevated range of costs. We developed a metamodel mapping afferent feedback signals to effort modulation using Partial Least Squares Regression (PLSR) as a dimensionality reduction technique. We also estimated the metabolic cost of transport (CoT) of walking using this PLSR metamodel. Furthermore, we predicted gait characteristics such as the economical speed (ES) using this estimated value of CoT. We validated our predictions using model accuracy metrics and statistical tests of significance. Our results indicate that the peripheral nervous system may regulate unperturbed gait through afferent feedback factors related to muscle force generation in skeletal muscles.

4.2 Conclusion

Here we have proposed 27 key afferent feedback signals based on proprioceptive feedback that could be used to model effort modulation during human gait. We have used a linear combination of afferent feedback signals arising from proprioceptive feedback to estimate the metabolic energy expenditure during walking. We have also shown that the musculoskeletal system might be tuned to maximise the economy of locomotion through key afferent factors

CHAPTER 5 : REFERENCES & BIBLIOGRAPHY

1. Abe, Daijiro, Fukuoka, Yoshiyuki, & Horiuchi, Masahiro. (2015, 09). Economical Speed and Energetically Optimal Transition Speed Evaluated by Gross and Net Oxygen Cost of Transport at Different Gradients. PloS one, 10, e0138154. 10.1371/journal.pone.0138154
2. af Klint, R., Mazzaro, N., & Nielsen JB, Sinkjaer T, Grey MJ. (2010). Load rather than length sensitive feedback contributes to soleus muscle activity during human treadmill walking. J Neurophysiol, 103, 2747–2756. 10.1152/jn.00547.2009.
3. Akay, T.; Murray, A.J. (2021). Relative Contribution of Proprioceptive and Vestibular Sensory Systems to Locomotion: Opportunities for Discovery in the Age of Molecular Science. Int. J. Mol. Sci., 22. https://doi.org/10.3390/ijms22031467
4. Amann, M., Proctor, L., Sebranek, J., Eldridge, M., & Pegelow DF, Dempsey JA. (2008). Somatosensory feedback from the limbs exerts inhibitory influences on central neural drive during whole body endurance exercise. Journal of applied physiology, 105(6), 1714-24.
5. Anderson, F., & Pandy, M. (1999). A Dynamic Optimization Solution for Vertical Jumping in Three Dimensions. Comput Methods Biomech Biomed Engin, 2(3), 201-231. 10.1080/10255849908907988
6. Barbosa, T., Vianna, L., & Fernandes IA, Prodel E, Rocha HNM, Garcia VP, et al. (2016). Intrathecal fentanyl abolishes the exaggerated blood pressure response to cycling in hypertensive men. The Journal of physiology, 594(3), 715-25.
7. Bertram, J.E. (2005). Constrained optimization in human walking: cost minimization and gait plasticity. ournal of experimental biology, 208.(6), 979-991.
8. Bhargava, L., Pandy, M., & Anderson, F. (2004, Jan). A phenomenological model for estimating metabolic energy consumption in muscle contraction. J Biomech, 37(1), 81-8. 10.1016/s0021-9290(03)00239-2

9. BL Luu, Day, B., & Cole JD, Fitzpatrick RC. (2011). The fusimotor and reafferent origin of the sense of force and weight. J Physiol, 589, 3135–3147. https://doi.org/10.1113/jphysiol.2011.208447
10. Brockway, J. M. (1987). Derivation of formulae used to calculate energy expenditure in man. Hum. Nutr. Clin. Nutr., 41, 463–471.
11. Capaday C, & Stein RB. (1986, May). Amplitude modulation of the soleus H-reflex in the human during walking and standing. J Neurosci., 6(5), 1308-13. 10.1523/JNEUROSCI.06-05-01308.1986
12. Carrier, D., Anders, C., & Schilling, N. (2011, Nov). The musculoskeletal system of humans is not tuned to maximize the economy of locomotion. Proc Natl Acad Sci U S A, 108(46), 18631-6. 10.1073/pnas.1105277108
13. Chow, G. C. (1960). Tests of Equality Between Sets of Coefficients in Two Linear Regressions. Econometrica, 3, 591-605. 10.2307/1910133
14. Delp, S., Loan, H., Hoy, M., Zajac, F., Topp, E., & Rosen, J. (1990). An interactive graphics-based model of the lower extremity to study orthopaedic surgical procedures. IEEE Trans Biomed Eng., 37(8), 757-767. 10.1109/10.102791
15. Di Russo, A., Stanev, D., Armand, S., & Ijspeert, A. (2021, May). Sensory modulation of gait characteristics in human locomotion: A neuromusculoskeletal modeling study. Plos Computational Biology. https://doi.org/10.1371/journal.pcbi.1008594
16. Donelan, J. M., Kram, R., & Kuo, A. D. (2002). Mechanical work for step-to-step transitions is a major determinant of the metabolic cost of human walking. J. Exp. Biol. 205, 3717–3727.
17. Faraji, S., Wu, A.R., & Ijspeert, A.J. (2018). A simple model of mechanical effects to estimate metabolic cost of human walking. Sci Rep, 8. https://doi.org/10.1038/s41598-018-29429-z
18. Fenn, W. (1924). The relation between the work performed and the energy liberated in muscular contraction. The Journal of physiology, 58, 373-395.
19. Gandevia, S. C., & McCloskey, D. (1977b). Changes in motor commands, as shown by changes in perceived heaviness, during partial curarization and peripheral anaesthesia in man. J. Physiol. (London), 272, 673-689.

20. Gandevia, S. C., & McCloskey, D. (1977a). Effects of related sensory inputs on motor performances in man studied through changes in perceived heaviness. J. Physiol. (London), 272, 653 -672.
21. Geijtenbeek, T. (2019). SCONE: Open Source Software for Predictive Simulation of Biological Motion. Journal of Open Source Software, 4(38), 1421. https://doi.org/10.21105/joss.01421
22. Geijtenbeek, T. (2021). The {Hyfydy} Simulation Software. https://hyfydy.com
23. Geyer H, Herr H. (2010, Jun). A muscle-reflex model that encodes principles of legged mechanics produces human walking dynamics and muscle activities. IEEE Trans Neural Syst Rehabil Eng, 18(3), 263-73. 10.1109/TNSRE.2010.2047592
24. Grey, M., Mazarro, N., & Nielsen JB, Sinkjaer T. (2004). Ankle extensor proprioceptors contribute to the enhancement of the soleus EMG during the stance phase of human walking. Can J Physiol Pharmacol, 82, 610–616. 10.1139/y04-077.
25. Griffin, T., Roberts, T., & Kram, R. (2003). Metabolic cost of generating muscular force in human walking: insights from load-carrying and speed experiments. Journal of Applied Physiology, 95(1), 172-83. 10.1152/japplphysiol.00944.2002
26. Hill, A. (1938). The heat of shortening and the dynamic constants of muscle. Proc R Soc Lond B Biol Sci, 126, 136-195.
27. Hunt, K. H., & Crossley, F.R.E. (1975). Coefficient of Restitution Interpreted as Damping in Vibroimpact. Journal of Applied Mechanics, 42(2), 440.
28. Ishikawa, M., Pakaslahti, J., & Komi, P.V. (2007). Medial gastrocnemius muscle behaviour during human running and walking. Gait Posture, 25, 308-384. 10.1016/j. gaitpost.2006.05.002
29. Kawato, M. (1999). Internal models for motor control and trajectory planning. Current Opinions in Neurobiology, 9, 718-727.
30. Ker, R. F., Alexander, R. M. & Bennet, M. B. (1988). Why are mammalian tendons so thick. J. Zool., 216, 309-324. 10.1111/j.1469-7998.1988.tb02432.x
31. Kjær, M., Secher, N., & Bach FW, Sheikh S, Galbo H. (1989). Hormonal and metabolic responses to exercise in humans: effect of sensory nervous blockade. American Journal of Physiology-Endocrinology And Metabolism, 257(1), E95-E101.
32. Kwak, S.T., & Chang, Y. (2023). Fascicle dynamics of the tibialis anterior muscle reflect whole-body walking economy. Sci Rep, 13(4660). 10.1038/s41598-023-31501-2

33. Lafargue, G., Paillard, J., Lamarre, Y., & Sirigu, A. (2003). Production and perception of grip force without proprioception: is there a sense of effort in deafferented subjects? Eur J Neurosci, 17, 2741–2749. https://doi.org/10.1046/j.1460-9568.2003.02700.x
34. Lajoie, Y., Teasdale, N., Cole, J.D., & ; Burnett, M.; Bard, C.; Fleury, M.; Forget, R.; Paillard, J.; Lamarre, Y. (1996). Gait of a deafferented subject without large myelinated sensory fibers below the neck. Neurology, 47, 109-115.
35. Lee, H. (2008, 09). Using the Chow Test to Analyze Regression Discontinuities. Tutorials in Quantitative Methods for Psychology, 4. 10.20982/tqmp.04.2.p046
36. Lichtwark, G. A. (2007). Muscle fascicle and series elastic element length changes along the length of the human gastrocnemius during walking and running. J. Biomech, 40, 157-164. 10. 1016/j.jbiomech.2005.10.035
37. Marsh, R., & Ellerby, D. (2006). Partitioning locomotor energy use among and within muscles: muscle blood flow as a measure of muscle oxygen consumption. J. Exp. Biol.
38. Miall, R., Weir, D., Wolpert, D., & Stein, J. (1993). Is the cerebellum a Smith Predictor? J Mot Behav, 25, 203–216.
39. Millard, M., Uchida, T., Seth, A., & Delp, S. L. (2013). Flexing computational muscle: modeling and simulation of musculotendon dynamics. Journal of Biomechanical Engineering, 135(2). https://doi.org/10.1115/1.4023390
40. Nielsen JB, & Sinkjaer T. (2002, Jun). Afferent feedback in the control of human gait. J Electromyogr Kinesiol., 12(3), 213-7. 10.1016/s1050-6411(02)00023-8
41. Ong CF, C., Geijtenbeek, T., Hick, J., & Delp, S. (2019). Predicting gait adaptations due to ankle plantarflexor muscle weakness and contracture using physics-based musculoskeletal simulations. PLoS Comput Biol., 7(15), 10. 10.1371/journal.pcbi.1006993
42. Oyedele, O. F., & Lubbe, S. (2015). The Construction of a Partial Least Squares Biplot. Journal of Applied Statistics, 42(11), 2449-2460.
43. Pierotti, D., Roy, R., & , Gregor RJ, Edgerton VR. (1989). Electromyographic activity of cat hindlimb flexors and extensors during locomotion at varying speeds and inclines. Brain Res, 481, 57–66. 10.1016/0006-8993(89)90485-X.

44. Praagman, M., Veeger HE, H., Chadwick, E., Colier WN, W., & van der Helm, F. (2003). Muscle oxygen consumption, determined by NIRS, in relation to external force and EMG. J Biomech, 36, 905–912.
45. Price, M., Huber, M., & Hoogkamer, W. (2023, Mar 8). Minimum effort simulations of split-belt treadmill walking exploit asymmetry to reduce metabolic energy expenditure. J Neurophysiol. 10.1152/jn.00343.2022
46. Reisman, D., Binder-MacLeod, S., & Farquhar, W. (2013, Mar-Apr). Changes in metabolic cost of transport following locomotor training poststroke. Top Stroke Rehabil, 20(2), 161-70. 10.1310/tsr2002-161
47. Roberts, T.J. (2002). The integrated function of muscles and tendons during locomotion. Comp. Biochem. Physiol. A, 133, 1087-1099. 10.1016/S1095-6433(02)00244-1
48. Rock, C., Marmelat, V., Yentes, J., Siu, K., & Takahashi, K. (2018, Nov). Interaction between step-to-step variability and metabolic cost of transport during human walking. J Exp Biol, 221(22). 10.1242/jeb.181834
49. Rubenson J, Heliams DB, Maloney SK, Withers PC, Lloyd DG, Fournier PA. Reappraisal of the comparative cost of human locomotion using gait-specific allometric analyses. J. Exp. Biol. 210:3513Y24. (2007).
50. Sanchez, N., Simha, S., Donelan, J., & Finley, J. (2019). Taking advantage of external mechanical work to reduce metabolic cost: the mechanics and energetics of split-belt treadmill walking. Journal of Physiology, 597, 4053-4068.
51. Sanchez, N., Simha, S., Donelan, J., & Finley, J. (2021). Using asymmetry to your advantage: Learning to acquire and accept external assistance during prolonged split-belt walking. Journal of Neurophysiology., 125, 344-357.
52. Sanes, J., & Shadmehr, R. (1995). Sense of muscular effort and somesthetic afferent information in humans. Can J Physiol Pharmacol, 73, 223–233. https://doi.org/10.1139/y95-033
53. Sawicki, G. S., Lewis, C. L. & Ferris, D. P. (2009). It pays to have a spring in your step. Exerc. Sport Sci. Rev., 37, 130-38. 10.1097/JES.0b013e31819c2df6
54. Selinger, J. C., O'Connor, S. M., & J. D. Wong, and J. M. Donelan. (2015, Sep). Humans Can Continuously Optimize Energetic Cost during Walking. Current Biology, 25(18), 2452–2456. 10.1016/j.cub.2015.08.016

55. Sinkjaer, T., Andersen, J., & Ladouceur M, Christensen LOD, Nielsen JB. (2000). Major role for sensory feedback in soleus EMG activity in the stance phase of walking in man. J Physiol, 523, 827-827. 10.1111/j.1469-7793.2000.00817.x.
56. Smith, N. P., Barclay, C. J., & Loiselle, D. S. (n.d.). The efficiency of muscle contraction. Progress in Biophysics and Molecular Biology, 88(1), 1-58. 10.1016/j.pbiomolbio.2003.11.014
57. Smith, S., Querry, R., & Fadel PJ, Gallagher KM, Strømstad M, Ide K, et al. (2003). Partial blockade of skeletal muscle somatosensory afferents attenuates baroreflex resetting during exercise in humans. The Journal of physiology., 551(3), 1013-21.
58. Taylor, C., Heglund, N., & Maloiy, G. (1982). Energetics and mechanics of terrestrial locomotion. I. Metabolic energy consumption as a function of speed and body size in birds and mammals. J. Exp. Biol., 97(1).
59. Uchida TK, Hicks JL, Dembia CL, & Delp SL. (2016). Stretching Your Energetic Budget: How Tendon Compliance Affects the Metabolic Cost of Running. PLoS One, 11(3). 10.1371/journal.pone.0150378
60. Umberger, B., Gerritsen, K., & Martin, P. (2003, Apr). A model of human muscle energy expenditure. Comput Methods Biomech Biomed Engin, 6(2), 99-111. 10.1080/1025584031000091678
61. Umberger, B., & Rubenson, J. (2011). Understanding muscle energetics in locomotion: new modeling and experimental approaches. Exercise and sport sciences reviews, 39(2), 59-67.
62. Wall, P.D.; Dubner, R. (1972). Somatosensory pathways. Annu. Rev. Physiol., 34, 315-336.
63. Wang, J., Hammer, S., Delp, S., & Koltun, V. (2012, Jul). Optimizing Locomotion Controllers Using Biologically-Based Actuators and Objectives. ACM Trans Graph, 31(4), 25. 10.1145/2185520.2185521
64. Waters, R., & Mulroy, S. (1999). The energy expenditure of normal and pathologic gait. Gait. Posture.
65. Wolpert, D., Miall, R., & Kawato, M. (1998). Internal models in the cerebellum. Trends in Cognitive Science, 2, 338-347.
66. Wong, J. D., O'Connor, S. M., Selinger, J. C., & Donelan, J. M. (2017). Contribution of blood oxygen and carbon dioxide sensing to the energetic optimization of human walking. Journal of Neurophysiology, 118(2), 1425-1433.

67. Yang JF, Stein RB, & James KB. (1991). Contribution of peripheral afferents to the activation of the soleus muscle during walking in humans. Exp Brain Res, 87(3), 679-87.
68. Zarrugh, M. Y., Todd, F. N. & Ralston, H. J. (1974). Optimization of energy expenditure during level walking. Eur. J. Appl. Physiol., 33, 293-306.

ACKNOWLEDGEMENT

I start by showing our gratitude to my project mentors, Professor Raju M. Tayade (V.J.T.I.), Professor Auke Ijspeert (EPFL, Switzerland) and Professor James Finley (USC) who have been a constant force in guiding us throughout the project, providing their vast acumen of knowledge wherever required. This project would not have been possible without the resources provided to us.

We would also like to thank the entire Mechanical EngineeringDepartment Staff for being supportive of our aspiration and facilitating its completion. We are eternally owed to the Society of Robotics and Automation, VJTI for being such a wonderful platform for us to bridge the gap between theoretical knowledge and practical experience.

If, in the course of acknowledging the contributors to the project, we have forgotten any names, generously pardon us.